Cell Transplantation, Vol. 22, pp. 1981–2000, 2013

0963-6897/13 $90.00 + .00
DOI: http://dx.doi.org/10.3727/096368912X657990
E-ISSN 1555-3892
www.cognizantcommunication.com

GMP-Compliant Isolation and Expansion of Bone Marrow-Derived MSCs in the Closed, Automated Device Quantum Cell Expansion System

Markus T. Rojewski,*†[1] Natalie Fekete,*†[1] Stefano Baila,‡ Kim Nguyen,§ Daniel Fürst,† Delbert Antwiler,§ Julia Dausend,* Ludwika Kreja,¶ Anita Ignatius,¶ Luc Sensebé,# and Hubert Schrezenmeier*†

*Institut für Transfusionsmedizin, Universität Ulm, Ulm, Germany
†Institut für klinische Transfusionsmedizin und Immungenetik Ulm, DRK-Blutspendedienst Baden-Württemberg – Hessen gemeinnützige GmbH, Ulm, Germany
‡Terumo BCT, Zaventem, Belgium
§Terumo BCT, Lakewood, CO, USA
¶Institute of Orthopaedic Research and Biomechanics, Center of Musculoskeletal Research, University of Ulm, Ulm, Germany
#EFS Pyrénées Méditerranée, Toulouse, France

The estimated frequency of MSCs in BM is about 0.001–0.01% of total nucleated cells. Most commonly, one applied therapeutic cell dose is about 1–5 million MSCs/kg body weight, necessitating a reliable, fast, and safe expansion system. The limited availability of MSCs demands for an extensive ex vivo amplification step to accumulate sufficient cell numbers. Human platelet lysate (PL) has proven to be a safe and feasible alternative to animal-derived serum as supplement for MSC cultivation. We have investigated the functionally closed automated cell culture hollow fiber bioreactor Quantum cell expansion system as an alternative novel tool to conventional tissue flasks for efficient clinical-scale MSC isolation and expansion from bone marrow using PL. Cells expanded in the Quantum system fulfilled MSC criteria as shown by flow cytometry and adipogenic, chondrogenic, and osteogenic differentiation capacity. Cell surface expression of a variety of chemokine receptors, adhesion molecules, and additional MSC markers was monitored for several passages by flow cytometry. The levels of critical media components like glucose and lactate were analyzed. PDGF-AA, PDGF-AB/BB, bFGF, TGF-β1, sICAM-1, sVCAM-1, RANTES, GRO, VEGF, sCD40L, and IL-6 were assessed using a LUMINEX platform. Originally optimized for the use of fetal calf serum (FCS) as supplement and fibronectin as coating reagent, we succeeded to obtain an average of more than 100×10^6 of MSCs from as little as 18.8–28.6 ml of BM aspirate using PL. We obtained similar yields of MSCs/µl BM in the FCS-containing and the xenogen-free expansion system. The Quantum system reliably produces a cellular therapeutic dose in a functionally closed system that requires minimal manipulation. Both isolation and expansion are possible using FCS or PL as supplement. Coating of the hollow fibers of the bioreactor is mandatory when loading MSCs. Fibronectin, PL, and human plasma may serve as coating reagents.

Key words: Mesenchymal stem cells (MSCs); Good manufacturing practice (GMP); Bioreactor; Large scale

INTRODUCTION

Mesenchymal stem cells (MSCs) are adult multipotent progenitor cells that are readily available from several human tissues and that have emerged as attractive candidates for cellular therapy. The hallmark characteristics as defined by the International Society for Cellular Therapy (ISCT) include plastic adherence, differentiation capacity along the mesenchymal lineages and a set panel of positive [cluster of differentiation 29 (CD29), CD44, CD73, CD90, CD105, CD166] and negative (CD14, CD31, CD34, CD45) surface markers (10). Depending on the stimuli and culture environment provided, MSCs can form bone, muscle, cartilage, or adipose tissue (25).

Their unique abilities to migrate to inflamed tissues and to establish a regenerative microenvironment by actively and specifically suppressing aberrant immune responses has generated profound interest in their clinical application. Putatively, these immunomodulatory effects

Received April 26, 2012; final acceptance September 20, 2012. Online prepub date: October 25, 2012.
[1]These authors provided equal contribution to this work.
Address correspondence to Markus T. Rojewski, Institut für Transfusionsmedizin, Universität Ulm, Helmholtzstraße 10, D-89081 Ulm, Germany. Tel: +49-7 31-1 50 68 33; Fax: +49-7 31-15 05 00; E-mail: markus.rojewski@uni-ulm.de

of MSCs rely on cell-to-cell contact-dependent interactions as well as on secreted factors shaping their immediate milieu.

In human bone marrow (BM), the frequency of MSCs is estimated to be about 0.001–0.01% of total nucleated cells and also has been reported to decline with age (8). Numerous clinical trials are currently registered at www.clinicaltrials.gov investigating the potential of MSCs in immune regulation, hematopoiesis, and tissue regeneration (7). Most commonly, one applied therapeutic cell dose is about 1–5 million MSCs/kg body weight (27), necessitating a reliable, fast, and safe ex vivo expansion system. The limited availability of MSCs is therefore a major concern regarding their clinical use. Moreover, as their clinical efficacy may depend on multiple doses given, an extensive ex vivo amplification step is necessary to accumulate sufficient cell numbers.

So far, no unique marker has been identified to be singularly suitable for prospective MSC isolation from BM, reflecting the heterogeneity of these cells (2). Also, current isolation protocols employed in laboratories still largely rely on plastic adherence of MSCs and greatly differ in their expansion methodologies (3).

Among the parameters that are crucial for efficient and reliable MSC expansion, the cells must be provided with growth factors, attachment, and spreading factors in their culture medium. While the regulatory agencies still tolerate the use of xenogeneic components in MSC culture, specially tailored animal-free cultivation systems will serve to consolidate the high level of health protection and offer an ethical advantage. Human platelet lysate (PL) generated from whole blood-derived pooled platelet concentrates has proven to be a safe and feasible alternative to animal-derived serum as supplement for MSC cultivation. PL has been shown to contain a multitude of bioactive components and allows for large-scale cell amplification in conventional tissue culture (12).

MSCs may be influenced differentially by variable concentrations of trophic molecules and their biological properties are presumably dictated by the local microenvironment.

Thus, controlling and optimizing MSC in vitro culture settings is paramount to guarantee a safe and economical cell expansion.

In this study, we investigated an automated cell culture bioreactor, the Quantum cell expansion system, as an alternative novel tool to conventional tissue flasks for efficient clinical-scale MSC isolation and expansion from BM. The Quantum system is a functionally closed, automated bioreactor system designed to cultivate both adherent and suspension cells. The culture system is comprised of a synthetic hollow fiber bioreactor that is part of a sterile closed-loop circuit for media and gas exchange.

The Quantum is a commercial product distributed by Terumo BCT. The system is optimized for expansion of adherent cells in medium containing fetal calf serum (FCS) (17). The aim of this collaborative study was the development of xeno-free cell culture processes that are compatible with this product.

MATERIALS AND METHODS

Six BM aspirates were either purchased from Lonza (Gaithersburg, MD, USA) or aspiration was performed from healthy volunteer donors (male and female, aged 23–27 years) at the Institut für klinische Transfusionsmedizin und Immungenetik Ulm (IKT Ulm) after informed consent according to the Declaration of Helsinki. The project was approved by the Ethical Committee of Ulm University.

Quantum® Cell Expansion System

The Quantum system (Terumo BCT, Lakewood, CO, USA) is a functionally closed, automated hollow fiber bioreactor system designed to grow both adherent and suspension cells. The bioreactor culture system is comprised of a synthetic hollow fiber bioreactor that is part of a sterile closed-loop circuit for media and gas exchange. The bioreactor and fluid circuit are a single-use disposable set that is mounted onto the Quantum system unit. The bioreactor itself is comprised of ~11,500 hollow fibers with a total intracapillary surface area of 2.1 m^2. With hollow fiber devices (HFBR, hollow fiber bioreactor), cells can be grown inside the hollow fibers [intracapillary (IC)], outside the fibers [extracapillary (EC)], or simultaneously on both sides. The Quantum system uses the inside of the fibers as the culture substrate. The total IC surface area is approximately equivalent to one 40-stack manual cell culture chamber. The hydraulic permeability and membrane sieving coefficient of the hollow fiber membrane is such that nutrients, metabolites, and gases easily diffuse across the fiber, while proteins and large macromolecular media components are retained on the IC side of the bioreactor.

Typical culture manipulations (e.g., cell seeding, media exchanges, trypsinization, cell harvest, etc.) are managed by the computer-controlled system using pumps and automated valves, which direct fluid through the disposable set and exchanges gas with the media. The functionally closed nature of the disposable set is maintained through the sterile docking of bags used for all fluids; these bag connections/disconnections all utilize sterile connection technology.

The Quantum system can perform operations ranging from a manual mode (custom task) to full automation of a specific process (automated task). Gas control in the system is managed using a hollow fiber oxygenator (gas transfer module). Premixed gas consisting of 5% CO_2 in 20% O_2 and 75% N_2 (MTI Industriegase, Neu-Ulm,

Germany) was used to grow MSCs. To allow the attachment of MSCs to the IC membrane, the inner side of the fibers were coated with at least either 100 ml of human plasma (IKT Ulm, Ulm, Germany), 100 ml of human platelet lysate (PL) (IKT Ulm), 10 mg of human fibronectin (BD Biosciences, Heidelberg, Germany) in PBS (Lonza, Basel, Switzerland), or 10 mg of poly-L-lysine (Sigma, Schnelldorf, Germany) in PBS, respectively. As opposed to traditional cell culture in flasks, the Quantum system provides a continual inlet of fresh media, while concurrently removing an equivalent volume of spent media. Over the course of an expansion in the Quantum system, the inlet rate of fresh media is typically increased up to 16-fold, as the cell population grows. Consequently, the concentration of any media component in the system is a function of the rate at which fresh media is added to the system, the rate at which media is removed from the system, and the rate at which the growing cell population generates or consumes the component. The bioreactor membrane between the IC and EC spaces allows free gas diffusion between the IC and EC sides of the bioreactor, as well as small molecule diffusion so that glucose and lactate freely pass from one side of the membrane to the other while larger macromolecules are sequestered on the side of the membrane in which they are added. Cells are grown utilizing the fresh complete media [90% minimum essential medium with α-modification (α-MEM; Lonza, Basel, Switzerland), supplemented with either 10% PL and 2 IU/ml of heparin (B. Braun, Melsungen, Germany) or 10% FCS (Gibco/Life Technologies, Freiburg, Germany), depending on the experimental setting] added to the IC side of the bioreactor and the IC inlet rate adjusted as required by the rate of glucose consumption and lactate generation in the system as sampled from the sample port twice daily. If glucose values are below 75 mg/dl in the morning or 85 mg/dl in the afternoon, the rate is increased twofold. Depending on the adjusted feed rates, medium exchanges rates varied from 6 to 144 ml/h. The IC waste valve is open for the duration of the expansion phase to allow waste media to collect into the waste bag and to prevent protein accumulation in the IC loop. The term "washout" refers to removal of nonadherent cells and/or complete medium exchange in the bioreactor. This process is comparable to complete medium exchange in a conventional tissue culture system.

Colony Assay and T-25 Parallel Culture

Colony assays were set up seeding nonmanipulated fresh BM in α-MEM supplemented with 10% PL within 6.5 h after BM collection at a mononuclear cell (MNC) density corresponding to the seeding density of the Quantum system. After 72 h, nonadherent cells were removed by washing with PBS without Ca^{2+}/Mg^{2+}. Medium exchange was performed twice per week. Colonies consisting of more than five cells were counted after 7 days of culture. Cells were further grown until harvesting cells from the Quantum system. Cell count was performed using trypan blue (Invitrogen, Darmstadt, Germany) to discriminate dead cells. Doubling time was determined on the base of colonies after 7 days using the following equation: doubling time (h) = ln(2) × culture time (h)/ln[total MSC number harvested/(number of colony forming unit-fibroblasts (CFU-F) × cell number seeded)]. Number of population doublings was determined as: number of population doublings = [time of culture (d) × 24 (h/d)]/doubling time (h). For parallel cultures in T-25 flasks (Thermo-Scientific, Nunc, Schwerte, Germany) of MSCs higher than passage 0, MSCs were seeded at the same density as in the Quantum system. Medium exchange was performed twice per week, and cells were harvested at the same day as for Quantum system.

Flow Cytometric Characterization

Antibodies used for characterization of MSCs included CD3 (SK7), CD9 (M-L13), CD34 (8G12), CD40 (5C3), CD45 (2D1), CD49a (SR84), CD49c (C3.11.1), CD49d (9F10), CD49f (GoH3), CD56 (NCAM16.2), CD71 (M-A712), CD73 (AD2), CD90 (5E10), human leukocyte antigen (HLA)-DR,DP,DQ (Tü39), HLA-ABC (G46-2.6), CD140a (αR1), CD140b (18A2), CD146 (P1H12), chemokine (C-C motif) ligand 5/regulated upon activation normal T-cell expressed and presumably secreted (CCL5/RANTES; 2D5) (all from Becton Dickinson, Heidelberg, Germany), CD105 (SN6) (AbDSerotec, Düsseldorf, Germany), CD49e (NKI-SAM-1), CD194/chemokine (C-C motif) receptor 4 (CCR4; TG6/CCR4), CD197/CCR7 (TG8/CCR7), chemokine C-X-C motif) receptor 4 (CXCR4; 12G5), CD349 (W3C4E11) (all from BioLegend, San Diego, CA, USA), CD271 (ME20.4-1.H4), mesenchymal stem cell antigen-1 (MSCA-1; W8B2) (both from Miltenyi Biotech., Bergisch Gladbach, Germany), CD117/c-kit (104D2) (Invitrogen, Darmstadt, Germany), CD191/CCR1 (141-2) (MBL, Nagano, Japan), CD166 (3A6) (Lifespan Biosciences Inc., Seattle, WA, USA), CD31 (WM59), CD51 (RMV-7), CD193/CCR3 (5E8-G9-B4), CD29 (TS2/16) (all from eBioscience, Frankfurt, Germany), CD195/CCR5 (T21/8), CD200 (325516), CXCR7 (358426), CD309/vascular endothelial growth factor receptor (VEGFR; 89106), stage-specific embryonic antigen 4 (SSEA-4; MC-813-70) (all from R&D Systems, Wiesbaden-Nordenstadt, Germany).

Cells (1×10^6) were incubated with the appropriate amount of antibody according to manufacturers' recommendations, washed with PBS without Ca^{2+}/Mg^{2+}, and relative fluorescence intensity of cells was then acquired using fluorescent activated cell sorter (FACS) Aria with FACS DIVA software (BD Immunocytometry Systems, Heidelberg, Germany). In addition, expression of CD3,

CD34, CD45, CD73, CD90, CD105, HLA ABC, and HLA-DQ,DP,DR was measured independently as duplicate acquisitions, using a FACScan with CellQuest 3.3 software (BD Immunocytometry Systems).

Differentiation Assays

For differentiation assays 2.75×10^3–10^4 cells per cm^2 were seeded and differentiation was induced according to the manufacturers' instructions (adipogenic differentiation medium from Lonza; chondrogenic and osteogenic differentiation media from Miltenyi). After differentiation, cells were fixed in 4% paraformaldehyde (Sigma) and osteogenic differentiation was detected showing alkaline phosphatase activity and by demonstrating mineralized matrix via von Kossa staining. Adipogenic differentiation was monitored by staining with a saturated Oil Red O solution (counterstaining with Meyer's hematoxylin). Chondrogenic differentiation was monitored by methylene blue staining. All reagents for staining were purchased from Sigma except for methylene blue (Merck, Darmstadt, Germany). Collagen type II was detected in paraffin sections of the pellet cultures by visualizing the binding of the primary antibody (polyclonal rabbit anti-human collagen type II antibody; Rockland Immunochemicals, Gilbertsville, PA, USA; 600-401-104-01) via the horseradish peroxidase (HRP) reaction (Goat HRP-Polymer Kit, Biocare Medical/Zytomed Systems GmbH, Berlin, Germany).

Real-Time Reverse Transcriptase Polymerase Chain Reaction (Real-Time RT-PCR) and Semiquantitative PCR

Quantitative effects on gene expression were examined as previously described (28). Specific primer pairs [see Table 2 of ref. (27) and below] were designed using published gene sequences (PubMed, NCBI Entrez Nucleotide Database) and synthesized by Thermo Electron Ulm (Ulm, Germany). Primer sequences for collagen type I were as follows: forward, 5′-TGACCTCAAGATGTGCCACT-3′ and reverse, 5′-ACCAGACATGCCTCTTGTCC-3′. The amount of each respective amplification product was determined relative to the housekeeping gene glyceraldehyde 3-phosphate dehydrogenase (GAPDH).

Normalized values of differentiated cells were compared to the control at day 0 for osteogenic differentiation.

Semiquantitative PCR was used to analyze adipogenic differentiation as previously described (28).

Lactate and Glucose Analysis

Lactate concentration in cell culture supernatant was measured using the Lactate Pro Blood Lactate Test Meter (ARKRAY Inc., Amstelveen, Netherlands) according to manufacturer's instructions. The Lactate Pro Test Strip has a measuring range of 0.8–23.3 mmol/L and this device conforms to the Directive 98/79/EC.

Analysis of glucose concentration in cell culture supernatant was performed using the Contour Blood Glucose Monitoring System (Bayer Vital GmbH, Leverkusen, Germany) which has a measuring range of 10–600 mg/dl following manufacturer's recommendations.

Cytokine Analysis

Custom-designed MILLIPLEX® Human Cytokine/Chemokine 96-well Plate Assays (Cat. #MPXCYTO-60K, #HNDG3-36K, #TGFB-64K-01, Millipore Corporation, Billerica, MA, USA) were used for the simultaneous quantification of human cytokines and chemokines of cell culture supernatants as per the manufacturer's specifications.

Cell culture supernatant samples were collected from fresh medium, pre- and post-washout and preharvest. At each time point, the aliquot was then stored at –80°C for simultaneous measurement via the MILLIPLEX Cytokine Assay. Samples were processed in a way that they did not differ in number of freezing/thawing cycles.

Data are expressed as mean ± standard deviation.

Testing for Microbial Contamination

Microbial testing of the starting material (300 µl BM in 20 ml of PBS) as well as of the final product [20 ml of cell culture supernatant before harvest enriched with harvested MSCs ($>1\times10^6$ cells)] was performed in accordance with the European Pharmacopeia 2.6.27 using aerobic (BacT/ALERT BPA, BioMérieux, Nürtingen, Germany) and anaerobic (BacT/ALERT BPN, BioMérieux) culture bottles in the BacT/ALERT 240 system from BioMérieux.

Endotoxin testing of culture supernatant at harvest was performed according to European Pharmacopeia 2.6.14 by L&S Labor (Bad Bocklet-Großenbrach, Germany) using a Limulus amoebocyte lysate (LAL) test.

Table 1A. Characterization of Starting Material ($n=6$)

Parameter	Time Between Collection and Culture (h)	Cell Count (WBCs/µl)	Fraction of MNCs (%)	Colonies per 10^6 MNCs	Total Aspiration Volume (ml)	Total Colonies Content per Aspiration
Mean	24	42.2×10^3	23.0	51	50	24.6×10^3
SD	3	12.6×10^3	3.5	27	0	6.7×10^3
Minimum	18	30.4×10^3	18.7	21	50	15.8×10^3
Maximum	30	61.9×10^3	27.9	86	50	34.1×10^3

SD, standard deviation; WBCs, white blood cells; MNCs, mononuclear cells.

Table 1B. Setup and Results on Isolation and Expansion of MSCs in Two-Step Bioreactor System Using Fibronectin as a Coating Reagent ($n=6$)

Protocol	Parameter	Cells* Seeded per Entity	Seeding Density (Cells/cm^2)	Days of Culture	MSCs Harvested/Entity	Harvesting Density (MSCs/cm^2)	Population Doublings	Doubling Time (h)	MSCs Harvested per ml BM Seeded
Step 1	Mean	238×10^6	11,233	13.0	39.5×10^6	1.9×10^3	10.4	28.3	1.6×10^3
(Passage 0)	SD	45×10^6	2,012	0.0	5.8×10^6	0.4×10^3	0.5	0.6	0.2×10^3
	Minimum	171×10^6	8,143	13.0	29.0×10^6	1.4×10^3	9.1	27.4	1.2×10^3
	Maximum	349×10^6	16,619	13.0	65.2×10^6	3.1×10^3	11.8	30.0	2.6×10^3
Step 2	Mean	20.2×10^6	960	4.9	155×10^6	7.4×10^3	3.0	39.2	12.4×10^3
(Passage 1)	SD	0.4×10^6	21	0.2	18.2×10^6	0.9×10^3	0.2	1.8	1.5×10^3
	Minimum	19.7×10^6	938	4.4	138×10^6	6.6×10^3	2.7	35.3	11.0×10^3
	Maximum	24.5×10^6	1,167	5.2	217×10^6	10.3×10^3	3.4	42.7	17.6×10^3
Steps 1 and 2	Mean	n/a	n/a	18.0	155.0×10^6	n/a	13.3	n/a	12.4×10^3
combined	SD	n/a	n/a	0.2	18.2×10^6	n/a	1.6	n/a	1.5×10^3
	Minimum	n/a	n/a	17.4	138×10^6	n/a	11.6	n/a	11.0×10^3
	Maximum	n/a	n/a	18.2	217×10^6	n/a	15.2	n/a	17.6×10^3

Characterization of bone marrow (BM) used for expansions [fetal calf serum (FCS) as supplement, fibronectin coating] in Quantum system and results for combined two-step mesenchymal stem cell (MSC) isolation and expansion in Quantum system. *MNC for passage 0; MSCs for passage 1. SD, standard deviation; n/a, not applicable.

RESULTS

Testing for Microbial Contamination and Karyotyping

Quantum-expanded MSCs were negative in BacT/ALERT testing and endotoxin concentration in preparations was less than 1 IU/ml. No clones with chromosomal abnormalities were found by karyotyping for all analyzed Quantum-expanded MSCs of passage 1 as well as for higher passages up to passage 6.

MSC Isolation and Expansion Using FCS as Supplement in a Quantum Cell Expansion System Coated With Human Fibronectin

The Quantum system was tested for its original use for expansion of MSCs using FCS as supplement and coating its hollow fibers with human fibronectin. To assess data on expanding MSCs using these standard conditions, MSCs were isolated from six individual BM donors. Characterization of the BM aspirates is described in Table 1A. Each bioreactor was coated with 10 mg of fibronectin that was dissolved in at least 50 ml of PBS. BM was loaded and grown in α-MEM, supplemented with 10% FCS. For passage 0: $238\times10^6\pm45\times10^6$ MNCs were seeded per Quantum (seeding density of 11,233±2,012 MNCs/cm^2). After 10.4±0.5 population doublings during 13.0±0.0 days of culture, cells were harvested at a density of $1.9\times10^3\pm0.4\times10^3$ MSCs/cm^2, resulting in a total of $39.5\times10^6\pm5.8\times10^6$ MSCs per Quantum (Table 1B). A maximum of 24.5×10^6 MSCs ($20.2\times10^6\pm0.4\times10^6$) from passage 0 was directly loaded on a fibronectin-coated Quantum. After 4.9±0.2 days (3.9±0.2 population doublings), MSCs were harvested at a density of $7.4\times10^3\pm0.9\times10^3$ MSCs/cm^2, resulting in a total of $155.0\times10^6\pm18.2\times10^6$ MSCs per Quantum. Doubling time for passage 1 was longer compared to passage 0 (39.2±1.8 h as compared to 28.3±0.6 h).

MSC Isolation and Expansion Using Platelet Lysate as Supplement and Coating Reagent in a Quantum Cell Expansion System

In this FCS-free system for isolation and expansion of MSCs, BM was loaded on a PL-coated bioreactor within 2.0±2.2 h after collection. Characterization of the BM aspirates is described in Table 2A. Each Quantum system was coated with at least 100 ml of PL. BM was loaded and grown in α-MEM, supplemented with 10% PL. For passage 0: $140\times10^6\pm33\times10^6$ MNCs were seeded per

Table 2A. Characterization of Starting Material ($n=6$)

Parameter	Time Between Collection and Culture (h)	Cell Count (WBCs/µl)	Fraction of MNCs (%)	Colonies per 10^6 MNCs	Total Aspiration Volume (ml)	Total Colonies Content per Aspiration
Mean	2.0	36.1×10^3	22.6	451	22.6	82.8×10^3
SD	2.2	14.3×10^3	4.1	230	4.2	53.0×10^3
Minimum	1.0	24.6×10^3	17.7	71	18.8	11.4×10^3
Maximum	6.5	57.9×10^3	28.1	698	28.6	146.0×10^3

SD, standard deviation.

Quantum (seeding density of 6,678 ± 1,581 MNCs/cm^2). After 8.8 ± 1.5 population doublings during 12.7 ± 2.2 days of culture, cells were harvested at a density of $1.4\times10^3 \pm 1.2\times10^3$ MSCs/cm^2, resulting in a total of $29.8\times10^6 \pm 25.0\times10^6$ MSCs per Quantum (Table 2B). A maximum of 20×10^6 MSCs ($14.4\times10^6 \pm 5.7\times10^6$) from passage 0 was directly loaded on a PL-coated Quantum. After 5.9 ± 0.6 days (2.9 ± 0.7 population doublings), MSCs were harvested at a density of $5.6\times10^3 \pm 2.8\times10^3$ MSCs/cm^2, resulting in a total of $118\times10^6 \pm 58.9\times10^6$ MSCs per Quantum. Doubling time for passage 1 was higher than for passage 0 (49.9 ± 12.5 h as compared to 35.0 ± 5.9 h). In parallel to this isolation and expansion of MSCs in a Quantum, cell culture in conventional T-25 flasks was performed (Table 2C). Both passage 0 and passage 1 of this small-scale parallel culture were comparable to the Quantum system regarding culture time (12.4 ± 2.0 days for passage 0; 5.9 ± 0,6 days for passage 1). However, doubling time was shorter (25.4 ± 5.0 for passage 0; 29.3 ± 4.2 for passage 1), resulting in a higher MSCs harvest/cm^2 ($22.2\times10^3 \pm 16.2\times10^3$ for passage 0; $22.6\times10^3 \pm 12.2\times10^6$ for passage 1).

The xenogen-free system gives a similar yield of MSCs/µl BM for passage 0 as compared to the system using FCS as the supplement and fibronectin as the coating reagent, in spite of the shorter population doubling time of the fibronectin-coated system. This apparent inconsistency is due to the fact that the CFU-F content of the BM loaded into the xenogen-free system was more than two times higher than that loaded into the fibronectin-coated system.

The combined passage 0 and passage 1 MSC yield per µl of BM seeded on the Quantum system ($12.0\times10^3 \pm 11.6\times10^3$) was about 1/100 of expansions in T-25 flasks ($1{,}159.8\times10^3 \pm 1{,}240.9\times10^3$).

Testing Alternatives for PL and Fibronectin as Coating Reagent

Quantum preexpanded MSCs of passages higher than passage 0 were loaded on a Quantum cell expansion system coated with at least 100 ml of PL or plasma or with 10 mg poly-L-lysine, respectively (Table 3). Whereas coating with poly-L-lysine did not successfully enable cell growth, PL coating resulted in slightly better number of population doublings and higher MSC densities at harvest than plasma coating (Table 3). MSCs grown in parallel cultures using uncoated T-25 cell culture flasks showed comparable growth characteristics.

Effect of Cryopreservation on MSC Growth in the Quantum Cell Expansion System

To address the question whether cryopreserved MSCs can directly be loaded onto a Quantum system after thawing, just-in-time preexpanded MSCs and cryopreserved MSCs were loaded on Quantum system simultaneously. In parallel, cultures in T-25 cell culture flasks were set up. As shown in Table 4, values for doubling time of cultures of cryopreserved MSCs were 1.4-fold higher than for freshly preexpanded MSCs in the Quantum system and 1.1-fold higher in T-25 cell culture flasks.

Phenotypical Characterization of MSCs Isolated and Expanded in the Quantum System

Cells harvested from the Quantum cell expansion system were analyzed via flow cytometry for the presence or absence of characteristic surface markers at passage 0, passage 1, or higher passages. As illustrated in Figure 1, the cell product at passage 0 still contained cells expressing CD45 (5.9 ± 8.1% positive cells) and HLA-DR (19.0 ± 30.6% positive cells). Conversely, levels of typical MSC

Table 2B. Setup and Results on Isolation and Expansion of MSCs in Two-Step Bioreactor System Using PL as Supplement and Coating Reagent ($n = 6$)

Protocol	Parameter	Cells* Seeded per Entity	Seeding Density (Cells/cm^2)	Days of Culture	MSCs Harvested/Entity	Harvesting Density (MSCs/cm^2)	Population Doublings	Doubling Time (h)	MSCs Harvested per ml BM Seeded
Step 1	Mean	140×10^6	6,678	12.7	29.8×10^6	1.4×10^3	8.8	35.0	1.7×10^3
(Passage 0)	SD	33×10^6	1,581	2.2	25.0×10^6	1.2×10^3	1.5	5.9	1.4×10^3
	Minimum	88×10^6	4,202	9.8	6.8×10^6	0.3×10^3	6.9	30.7	0.3×10^3
	Maximum	182×10^6	8,676	14.9	70.6×10^6	3.4×10^3	10.5	46.7	4.0×10^3
Step 2	Mean	14.4×10^6	686	5.9	118.0×10^6	5.6×10^3	2.9	49.9	12.0×10^3
(Passage 1)	SD	5.7×10^6	270	0.6	58.9×10^6	2.8×10^3	0.7	12.5	11.6×10^3
	Minimum	6.6×10^6	313	4.9	32.8×10^6	1.6×10^3	2.3	32.6	1.4×10^3
	Maximum	20.0×10^6	952	6.9	195.5×10^6	9.3×10^3	4.3	71.0	32.8×10^3
Steps 1 and 2	Mean	n/a	n/a	18.5	118.0×10^6	n/a	11.7	n/a	12.0×10^3
combined	SD	n/a	n/a	2.3	58.9×10^6	n/a	2.1	n/a	11.6×10^3
	Minimum	n/a	n/a	14.7	32.8×10^6	n/a	9.2	n/a	1.4×10^3
	Maximum	n/a	n/a	20.8	195.5×10^6	n/a	14.6	n/a	32.8×10^3

*MNC for passage 0; MSCs for passage 1. SD, standard deviation; n/a, not applicable.

Table 2C. Setup and Results on T-25-Flask Parallel Culture ($n=6$)

Protocol	Parameter	Cells* Seeded per Entity	Seeding Density (Cells/cm^2)	Days of Culture	MSCs Harvested/Entity	Harvesting Density (MSCs/cm^2)	Population Doublings	Doubling Time (h)	MSCs Harvested per ml BM Seeded
Step 1	Mean	167×10^3	6,678	12.4	557.2×10^3	22.2×10^3	12.1	25.4	28.0×10^3
(Passage 0)	SD	40×10^3	1,581	2.0	404.5×10^3	16.2×10^3	3.2	5.0	20.0×10^3
	Minimum	105×10^3	4,202	9.8	7.2×10^3	0.3×10^3	6.7	20.8	0.3×10^3
	Maximum	217×10^3	8,676	14.0	$1{,}007.5\times10^3$	40.4×10^3	15.9	35.1	53.0×10^3
Step 2	Mean	17.2×10^3	686	5.9	564.9×10^3	22.6×10^3	4.9	29.3	$1{,}159.8\times10^3$
(Passage 1)	SD	6.7×10^3	270	0.6	306.7×10^3	12.2×10^3	1.0	4.2	$1{,}240.9\times10^3$
	Minimum	7.8×10^3	313	5.0	186.3×10^3	7.4×10^3	3.6	22.0	968.5×10^3
	Maximum	23.8×10^3	952	6.9	$1{,}000.0\times10^3$	40.0×10^3	6.4	33.3	$3{,}168.8\times10^3$
Steps 1 and 2	Mean	n/a	n/a	18.3	564.9×10^3	n/a	17.1	n/a	$1{,}159.8\times10^3$
combined	SD	n/a	n/a	2.1	306.7×10^3	n/a	3.6	n/a	$1{,}240.9\times10^3$
	Minimum	n/a	n/a	14.9	186.3×10^3	n/a	12.0	n/a	968.5×10^3
	Maximum	n/a	n/a	19.8	$1{,}000.0\times10^3$	n/a	22.3	n/a	$3{,}168.8\times10^3$

*MNCs for passage 0; MSCs for passage 1. SD, standard deviation; n/a, not applicable.

markers used for quality control of the final cell product, for example, CD73 (78.1±23.6% positive cells) and CD90 (89.6±17.7% positive cells), did not meet release criteria. However, cells harvested at passage 1 then showed negligible expression of CD3, CD34, CD45, and HLA-DR,DP,DQ as well as expectedly high levels of CD73, CD90, CD105, and HLA-ABC. This expression profile could also be observed in subsequent passages, allowing for the conclusion that the final cell product obtained at passage 1 or >1 presents a harmonized cell population meeting standard phenotypic criteria for MSCs.

MSC Differentiation Potential

Adipogenic, chondrogenic, and osteogenic differentiation of MSCs isolated and expanded in Quantum system using PL or plasma as coating reagent was successful (Figs. 2 and 3).

Chondrogenic differentiation was also confirmed immunocytochemically via collagen type II staining in paraffin sections of pellet cultures (Fig. 3B).

In addition to these histochemical stainings for visualizing the characteristic differentiation capacities, adipogenic and osteogenic differentiation potential analyzed in greater detail. Therefore, we investigated mRNA expression of osteogenic markers bone sialo protein (BSP), alkaline phosphatase (AP), osteopontin (OP), osteocalcin (OC), transcription factor runt-related transcription factor 2 (Runx2), and collagen type I in MSCs from two donors cultured under osteogenic conditions via quantitative RT-PCR and analyzed adipogenic differentiation by semiquantitative RT-PCR for lipoprotein lipase (LPL) and peroxisome proliferator activated receptor-γ (PPAR-γ). As illustrated in Figure 4, we observed a marked donor-dependent variability in the expression profile of BSP, AP, OP, and OC at day 0 and day 21 following induction of osteogenic differentiation. However, a distinct induction of expression could be detected for any of these osteogenic markers. In contrast, Runx2 and collagen type I expression showed little donor-dependent variation in their expression but failed to show a clear upregulation relative to controls (mRNA at day 0). Regarding adipogenic differentiation markers, we could detect a clear upregulation of both LPL and PPAR-γ (Fig. 5).

Extended Surface Marker Phenotype of MSCs Cultivated in the Quantum Cell Expansion System

In addition to the quality control markers defining MSCs according to standard guidelines, we also analyzed a multitude of further MSC surface antigens via flow cytometry (Figs. 6 and 7) to investigate possible functional properties of these cells. Our panel included chemokine receptors (CCRs) (e.g., CD191/CCR1, CD193/CCR3, CD194/CCR4, CD195/CCR5, CD197/CCR7, CXCR4, CXCR7), adhesion molecules (e.g., CD29/integrin β1, CD49a/integrin α1, CD49c/integrin α3, CD49d/integrin α4, CD49e/fibronectin receptor/integrin α5, CD49f/integrin α6, CD51/integrin αν, as well as a variety of extended markers [e.g., CD9, CD31/platelet endothelial cell adhesion molecule 1 (PECAM-1), CD56/neural cell adhesion molecule (NCAM), CD71/transferrin receptor, CD117/c-kit, CD140a/platelet-derived growth factor (PDGF) receptor α, CD140b/PDGF receptor β, CD146/melanoma cell adhesion molecule (MCAM), CD166/activated leukocyte cell adhesion molecule (ALCAM), CD200, CD271/nerve growth factor receptor (NGFR), CD309/VEGFR, CD349/frizzled homolog 9, CCL5/RANTES, MSCA-1 and SSEA-4]. This extensive analysis revealed considerable variability reflecting the well-known heterogeneity of MSCs. Whereas CCR1, CCR3, and CXCR7 could be observed to be downregulated by passaging of the cells,

Table 3. Expansion of MSCs ($p > 1$) Using Different Coating Reagents for Bioreactor System and PL as Supplement and Parallel Culture in T-25 Flasks Using PL as Supplement

		Quantum						T-25					
Coating	Parameter	Seeding Density (Cells/cm^2)	Days of Culture	MSCs Harvested/ Entity	Harvesting Density (MSCs/cm^2)	Population Doublings	Doubling Time (h)	Seeding Density (Cells/cm^2)	Days of Culture	MSCs Harvested/ Entity	Harvesting Density (MSCs/cm^2)	Population Doublings	Doubling Time (h)
PL	Mean	937	5.7	100.3×10^6	4.8×10^3	2.2	66.3	920	5.7	556.3×10^3	25.4×10^3	4.6	30.5
($n=26$)	SD	41	0.5	4.0×10^6	1.9×10^3	0.6	22.7	101	0.5	333.0×10^3	13.2×10^3	0.8	6.2
	Minimum	785	4.8	4.3×10^6	2.0×10^3	1.1	40.6	460	4.8	23.8×10^3	6.6×10^3	2.8	23.6
	Maximum	952	7.0	195.3×10^6	9.3×10^3	3.3	120.8	960	7.1	1530.9×10^3	61.2×10^3	6.0	50.2
Plasma	Mean	959	6.2	79.0×10^6	3.8×10^3	1.9	82.5	964	6.0	387.6×10^3	15.5×10^3	4.0	35.7
($n=3$*)	SD	12	0.5	28.5×10^6	1.4×10^3	0.6	23.1	12	0.2	30.0×10^3	1.2×10^3	0.1	0.1
	Minimum	952	5.8	49.5×10^6	2.4×10^3	1.3	67.2	956	5.8	366.4×10^3	14.7×10^3	3.9	35.6
	Maximum	973	6.8	106.4×10^6	5.1×10^3	2.4	169.1	973	6.1	408.8×10^3	16.4×10^3	4.1	35.7
10 mg	Mean	952	5.4	2.0×10^6	94.9	n/a	n/a	952	5.4	472.8×10^3	18.9×10^3	4.2	30.7
poly-	SD	0	0.6	0.5×10^6	24.8	n/a	n/a	0	0.6	206.3×10^3	8.3×10^3	0.7	1.5
L-lysine	Minimum	952	4.9	1.6×10^6	77.4	n/a	n/a	952	5.0	326.9×10^3	13.1×10^3	3.8	29.6
($n=2$)	Maximum	952	5.8	2.4×10^6	112.4	n/a	n/a	952	5.8	618.6×10^3	24.8×10^3	4.7	31.8

*$n=2$ for T-25 flasks. SD, standard deviation; n/a, not applicable; PL, platelet lysate.

Table 4. Expansion of MSCs ($p \geq 1$) in Bioreactor System and Parallel Culture in T-25 Flasks Using PL as Supplement Comparing Cryopreserved and Freshly Preexpanded MSCs as Starting Material

		Quantum						T-25					
	Parameter	Seeding Density (Cells/cm^2)	Days of Culture	MSCs Harvested/ Entity	Harvesting Density (MSCs/cm^2)	Population Doublings	Doubling Time (h)	Seeding Density (Cells/cm^2)	Days of Culture	MSCs Harvested/ Entity	Harvesting Density (MSCs/cm^2)	Population Doublings	Doubling Time (h)
Freshly	Mean	775	5.8	122.1×10^6	5.8×10^3	2.9	49.9	775	5.8	747.5×10^3	29.9×10^3	5.1	27.7
pre-	SD	251	0.6	49.1×10^6	2.3×10^3	0.6	10.0	251	0.6	418.6×10^3	16.7×10^3	0.8	4.2
expanded	Minimum	313	4.9	32.8×10^6	1.6×10^3	2.3	32.6	313	4.9	186.3×10^3	7.5×10^3	3.6	22.0
($n=9$)	Maximum	952	6.9	195.5×10^6	9.3×10^3	4.3	71.0	952	6.9	153.1×10^3	61.2×10^3	6.4	33.3
Cryo-	Mean	935	5.7	96.4×10^6	4.6×10^3	2.2	66.4	916	5.7	527.5×10^3	22.9×10^3	4.5	31.3
preserved	SD	44	0.5	40.3×10^6	1.9×10^3	0.6	23.3	107	0.5	210.1×10^3	10.8×10^3	0.7	6.1
($n=23$)	Minimum	785	4.8	43.0×10^6	2.0×10^3	1.1	40.6	460	4.8	164.0×10^3	6.6×10^3	2.8	24.1
	Maximum	952	7.0	195.3×10^6	9.3×10^3	3.3	126.8	960	7.1	1159.0×10^3	54.0×10^3	5.8	50.2

SD, standard deviation.

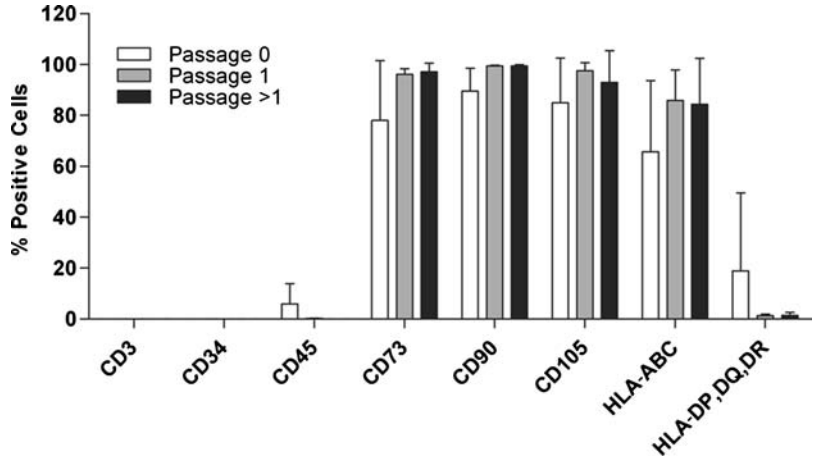

Figure 1. Flow cytometric analysis of quality control surface markers. Shown are mean and SD values of percent positive mesenchymal stem cells (MSCs) isolated and expanded in the bioreactor at passage 0, passage 1, and higher passages (passage >1). CD, cluster of differentiation; HLA, human leukocyte antigen.

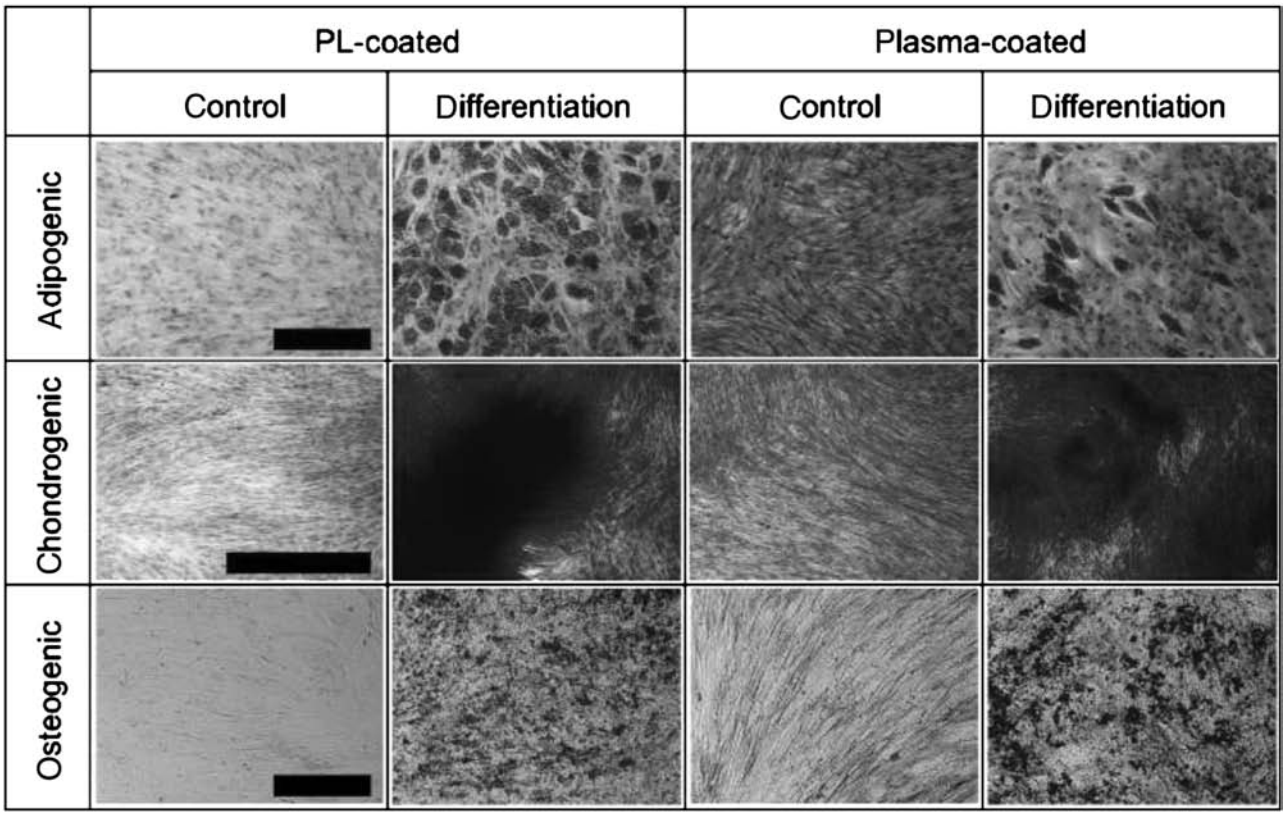

Figure 2. Differentiation capacity. Differentiation of representative batches of MSCs isolated and expanded using a Quantum cell expansion system on a bioreactor coated with 100 ml of platelet lysate (PL) or 100 ml of human plasma. Adipogenic (Oil Red O/hematoxylin staining), chondrogenic (methylene blue staining), and osteogenic (detection of alkaline phosphatase) differentiation assays are shown. Control assays were performed in mimumim essential medium with α-modification (α-MEM) supplemented with 10% fetal calf serum (FCS). Scale bars: 1,000 μm for adipogenic and 100 μm for chondrogenic and osteogenic differentiation.

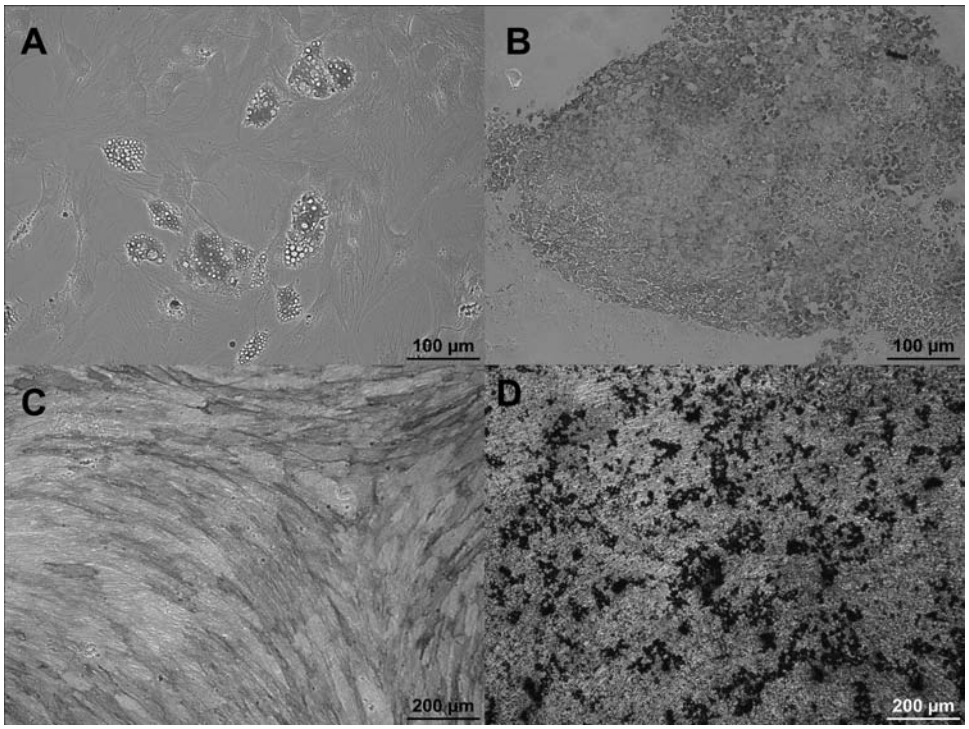

Figure 3. Differentiation of MSCs. (A) Oil Red O staining, (C) alkaline phosphatase detection, and (D) von Kossa staining for detection of adipogenic (A) or osteogenic (C, D) differentiation. (B) Paraffin section of the pellet culture at day 28 under chondrogenic conditions showing differentiated chondrocytes stained with antibody against collagen type II and counterstained with hematoxylin. The positive location of collagen type II was revealed by the immunoperoxidase reaction product.

two other chemokine receptors, CCR4 and CCR7, were found to be upregulated in the population in higher passages. Expression of CCR5 was found to be low and showed variable expression levels.

Similarly, expression of integrins, such as integrin $\alpha 1$, $\alpha 6$, and αv showed greater variation. However, integrin $\beta 1$, $\alpha 3$, and $\alpha 5$ appeared to be expressed on nearly 100% of all MSCs following passage 0, further indicating contamination of MSCs by cells of other lineages following isolation from the bone marrow. Interestingly, PDGF receptor α could only be detected at levels below 5.4% maximum expression, whereas PDGF receptor β was expressed at variable, but higher ($\geq$18.9% median expression) levels. Also, MSCA-1 and CD271, which are two markers suggested to be present only on early, undifferentiated MSCs, were found to be downregulated by passaging of MSCs, further confirming their status as possible candidates for prospective isolation of MSCs from bone marrow. Similarly, c-kit/CD117 showed high expression at passage 0 but decreased in expression at passages >1. CD200 was expressed at very low levels in passage 0 and in passage 1 but was then found to have high and variable expression (range 0.3–87.5% expression) following passage 1. Furthermore, CD349 expression increased from passage 0 to passage 1 and then declined at higher passages. Finally, median expression of SSEA-4 increased from passage 0 to passages>1, suggesting that this marker may only be present on a subpopulation of MSCs.

Altogether, the cells harvested from the bioreactor at passages 0, 1, and higher show pronounced variability in their surface receptor expression profile, indicating a multilayered effect of the cultivation system and passaging on the cell phenotype, representing an inhomogeneous MSC population as also observed in the in flask culture systems.

We also analyzed median fluorescence intensity for the same panel of surface markers of MSCs isolated and expanded in the bioreactor. Figure 7 illustrates the median fluorescence intensity of cells expressing the marker. The majority of markers show stable (CD9, CD29, CD140a, CD146, CD166, CD191, RANTES) or decreasing (CD31, CD40, CD49a, CD49d, CD49f, CD71, CD117, CD140b, CD193, CD195, CD197, CD200, CD271, CD309, CD349, CXCR4, CXCR7, MSCA-1) median fluorescence intensities. Inversely, CD29, CD49c, and CD56 show increasing MFI values, whereas CD49e, CD51, CD140a, CD194, and SSEA-4 show variable fluorescence intensities. These results suggest that overall surface antigen expression shows little variation in its intensity.

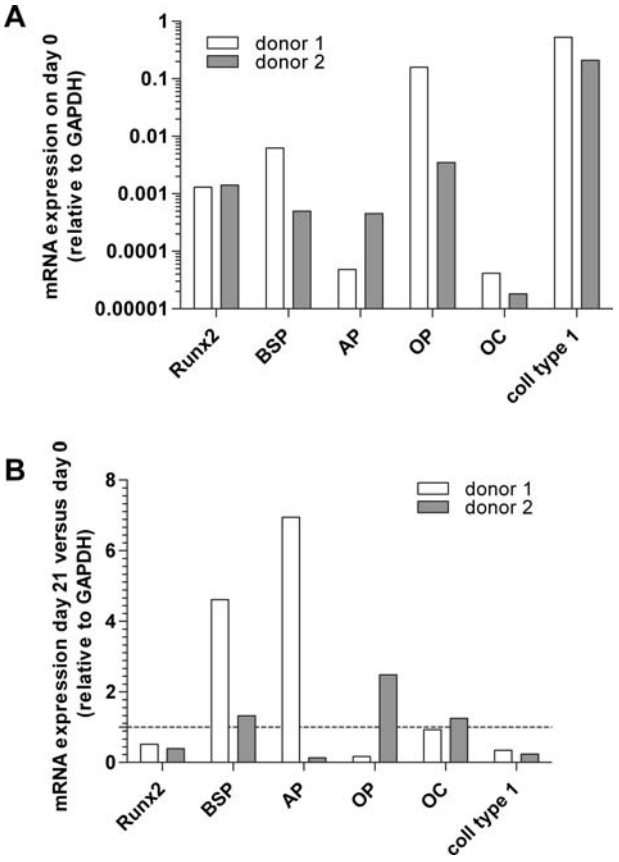

Figure 4. Expression of osteogenic markers in MSCs during differentiation. mRNA expression of the osteogenic markers bone sialo protein (BSP), alkaline phosphatase (AP), osteopontin (OP), osteocalcin (OC), collagen type I (coll type I), and transcription factor runt-related transcription factor 2 (Runx2) in MSCs from two donors cultured in osteogenic conditions was quantitatively measured and normalized to housekeeping gene glyceraldehyde 3-phosphate dehydrogenase (GAPDH) levels. (A) Relative mRNA expression of two MSCs donors on day 0. (B) Relative mRNA expression on day 21 versus day 0. Dotted bar indicates control value (mRNA at day 0 was set at 1).

Quantification of Soluble Cytokines in MSC Culture Medium in the Bioreactor of the Quantum Cell Expansion System

Since media and waste components pass through the porous membranes, creating a putatively stable and controlled microenvironment for cell cultivation, we were then interested in investigating the cytokine content of cell culture media within the bioreactor of the Quantum system. To this end, we collected media samples via the EC sample port after addition of fresh medium, pre- and post-washouts and just before harvesting the cells. These samples reflect the cell culture media composition as a result of supplemental factors as well as cellular secreted molecules. In addition, we simultaneously measured glucose consumption and lactate production to determine the metabolic state of the MSCs in culture. Regarding the latter, we could well observe an approximate correlation between glucose consumption for preexpanded MSCs, which declined from 86±6 g/L after cell seeding in fresh medium to 77±4 g/L just before harvest and lactate levels, which increased from 1.4±0.2 mM to 3.0±0.2 mM, respectively (Fig. 8). Quantification of PDGF-AA revealed stable amounts ranging from 3,443±723 pg/ml to 4,924±1,193 pg/ml, whereas PDGF-AB/BB levels first increased from 7,023±1,097 pg/ml in fresh medium to 9,609±1,007 pg/ml post-washout on day 1, but then decreased to 3,399±699 pg/ml preharvest. A similar pattern could be observed for soluble intercellular adhesion molecule 1 (sICAM-1), which increased starting from 1,676±273 pg/ml in fresh medium to 2,876±258 pg/ml post-washout and finally decreased to 1,530±312 pg/ml preharvest. In contrast, levels of soluble vascular cell adhesion molecule 1 (sVCAM-1) strongly decreased from 35,977±6,183 pg/ml in fresh medium to 1,1461±11,068 pg/ml pre-washout on day 1 and then increased post-washout to 29,547±3,739 pg/ml before harvest. The same inverse pattern could also be shown for RANTES (60,502±11,378 pg/ml in fresh medium, 13,235±8,138 pg/ml pre-washout day 1, 50,652±6,319 pg/ml preharvest) and transforming growth factor (TGF)-β1 (6,775±4,351 pg/ml in fresh medium, 2,419±763 pg/ml pre-washout day 1, 9,998±1,021 pg/ml preharvest). A similar, if less pronounced profile was also observed for growth-regulated oncogene (GRO; =CXCL1/2/3) (1,220±57 pg/ml in fresh medium, 1,040±63 pg/ml pre-washout day 1 and 1,192±51 pg/ml preharvest), basic fibroblast growth factor (bFGF; 137±28 pg/ml in fresh medium, 110±22 pg/ml pre-washout day 1 and 98±1 pg/ml preharvest), and VEGF (170±30 pg/ml in fresh medium, 93±21 pg/ml pre-washout day 1 and 189±34 pg/ml preharvest). Quantification of soluble CD40 ligand (sCD40L) revealed marked variability between individual runs, yet a strong decrease from 2,155±1,956 pg/ml in fresh medium to 581±498 pg/ml before harvest. Interestingly, levels of interleukin-6 (IL-6) were below the detection range in fresh medium, but then showed a strong increase to 120±49 pg/ml preharvesting (Fig. 8).

These analyzed runs were based on MSCs that had previously been isolated and expanded in the Quantum cell expansion system and were either directly transferred from a previous run into the bioreactor or had been cryogenically preserved at –80°C. To exclude any potential effect of cryostorage on MSC biology regarding cytokine consumption and secretion, we also analyzed the cytokine quantifications of "fresh" and "frozen" MSCs. As depicted in Figure 9, we could not observe marked variation in the overall cytokine level profile of cells that had previously been frozen compared to MSCs directly

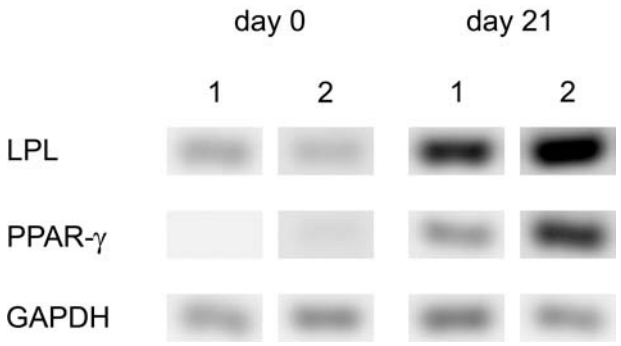

Figure 5. Expression of adipogenic markers in MSCs during differentiation. mRNA expression of GAPDH and the adipogenic differentiation marker genes lipoprotein lipase (LPL) and peroxisome proliferator activated receptor-γ (PPAR-γ) in undifferentiated MSCs from two donors (1, 2) at day 0 and in MSCs under adipogenic differentiation conditions at day 21.

transferred from a previous cultivation in the Quantum cell expansion system.

In addition, we then quantified cytokine and metabolite concentrations of bone marrow-derived cell culture at passage 0 (Fig. 10). Here, the glucose concentration decreased from 84±3 mg/dl in fresh medium to 75±2 mg/dl before the first washout. Conversely, lactate content showed a strong reciprocal increase from 1.53±0.21 to 3.60±0.17 mM at this time point. Subsequently, however, both glucose and lactate levels were comparable to their starting values (80±3 mg/dl glucose and 2.10±0.26 mM lactate before harvest) and did not show marked variation until the cells were harvested. The cytokine profile of cells isolated from the bone marrow in passage 0 followed the same general pattern compared to those at passage 1 or higher but exhibited greater variability that was especially marked before and after the first washout (Fig. 10). These results collectively reveal the metabolic state of proliferating cells in the bioreactor system and offer a unique insight into the complex continuum of cytokines being consumed and secreted by MSCs during in vitro cultivation.

DISCUSSION

Herein we present a comprehensive analysis of BM-derived MSCs isolated and expanded using a bioreactor system. Quantum system's bioreactor is comprised of thousands of hollow fibers, providing a large surface area for cell attachment in a compact space. Media and waste components pass through the porous membranes while a gas transfer module regulates gas concentration, making this bioreactor a functionally closed system with less risk of contamination and better control of the process.

In the context of regulations in the European Union, MSCs are now classified as an advanced therapy medicinal product (ATMP). Therefore, clinical-scale manufacture of MSCs must be performed according to the good manufacturing practice (GMP) for medicinal products. Specially tailored and harmonized rules regarding the production process as well as the biosafety and efficacy of its components have been issued by the European Medicines Agency (EMA) to guarantee optimal health protection.

During the stages of the manufacturing process, the risk of cross-contamination between medicinal products also requires additional precautions, for example, dedicated facilities and the use of closed systems. A closed system allowing for continuous monitoring of the production process can be considered highly advantageous, since in-process controls play an important role in ensuring the consistency of the quality of biological medicinal products. Also, minimal manipulation of the product as well as cell culture media and supplements of human or synthetic origin are recommended by the regulatory authorities.

Therefore, a special focus within this study was set on establishing a xenogenic free, functionally closed system and reduction of manipulating steps starting from an optimized system using FCS as supplement for growth. As we could show, we succeeded with this xenogenic free expansion system to obtain an average of more than 100×10^6 of MSCs from as little as 18.8 to 28.6 ml of BM aspirate. This amount of MSCs can be regarded as a clinical dose (27). We obtained similar yields of MSCs per µl BM in the FCS-containing and the xenogenic-free expansion system.

Moreover, we show that cells at passage 1 or higher that had been isolated and expanded from bone marrow via the Quantum system using human PL both for bioreactor coating and as cell media supplement are bona fide MSCs according to the characterization standards defined by the ISCT. They are plastic adherent cells expressing the minimal marker set of CD90, CD73, CD105, and HLA-ABC and absence of CD3, CD34, CD45, and HLA-DR. We have comprehensively documented adipogenic, chondrogenic, and osteogenic differentiation capacity of MSCs isolated and expanded in the Quantum system using PL or plasma as coating reagent via histochemical stainings and RT-PCR. The mRNA expression analysis revealed marked donor-dependent variability in the expression profile of osteogenic markers as previously reported (19,24).

The phenotypic analysis of MSC surface receptor profile via flow cytometry allowed us to determine the heterogeneity of cells isolated and expanded from bone marrow in the Quantum system. This assessment revealed a considerable number of contaminating cells expressing CD31, CD45, and HLA-DR present in the cells harvested at the end of passage 0. Conversely, expression of typical MSC markers CD29, CD73, CD90, CD105, and CD166

was found to be below 95% of the total cell population, which therefore does not meet the ISCT standards for MSCs.

However, cells that were further cultivated in the Quantum cell expansion system then displayed a more uniform surface marker profile characteristic of MSCs and conform to the ISCT criteria. MSCs harvested at the end of passage 1 or higher showed ≥95% expression of CD9, CD29, CD73, CD90, CD105, CD166, and HLA-ABC and ≤5% expression of CD3, CD31, CD34, CD45, and HLA-DP, DQ, DR. We also investigated the presence of putative surface markers suggested for prospective MSC isolation from BM. Subsequent passaging of cells in the Quantum system resulted in decreasing expression

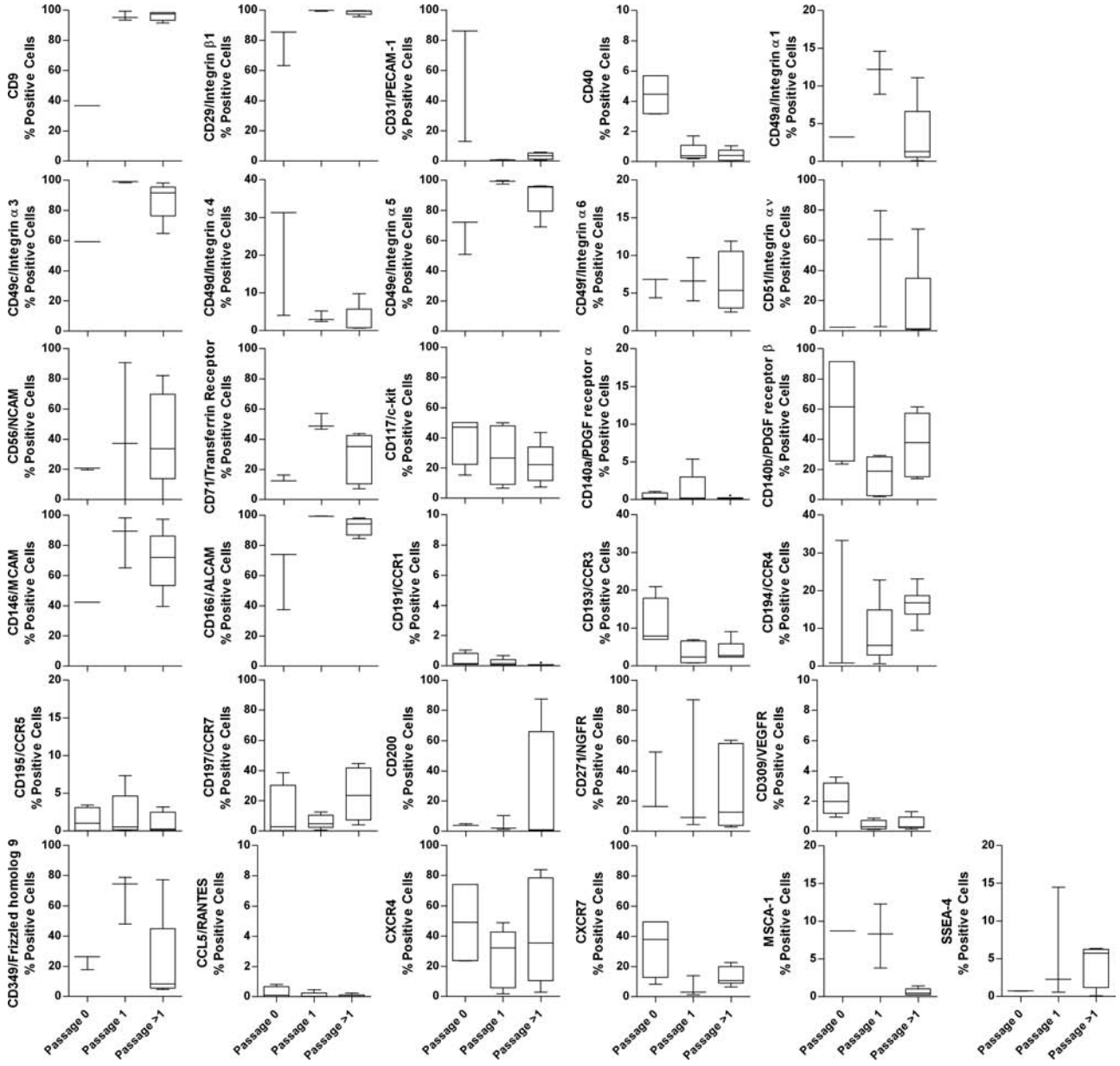

Figure 6. Flow cytometric analysis of extended surface marker antigens. Shown are percent positive cells of MSCs isolated and expanded in the bioreactor at passage 0, passage 1, and higher passages (passage >1) in whisker plots. PECAM-1, platelet endothelial cell adhesion molecule 1; NCAM, neural cell adhesion molecule; PDGF, platelet-derived growth factor; MCAM, melanoma cell adhesion molecule; ALCAM, activated leukocyte cell adhesion molecule; CCR1, chemokine (C-C motif) receptor 1; NGFR, nerve growth factor receptor; VEGFR, vascular endothelial growth factor receptor; CCL5, chemokine (C-C motif) ligand 5; RANTES, regulated upon activation normal T-cell expressed and presumably secreted; CXCR4, chemokine (C-X-C motif) receptor 4; MSCA-1, mesenchymal stem cell antigen-1; SSEA-4, stage-specific embryonic antigen 4.

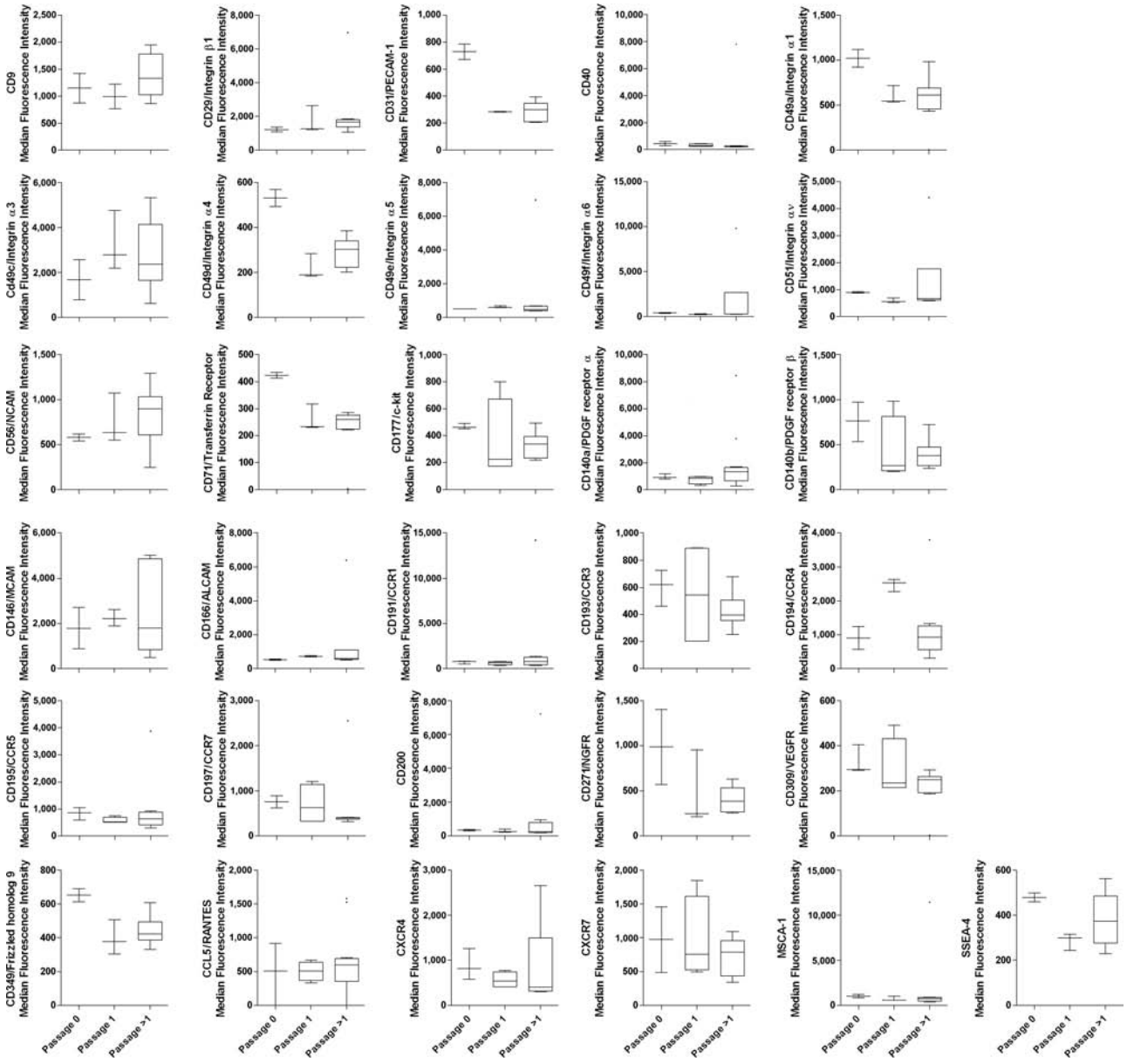

Figure 7. Flow cytometric analysis of extended surface marker antigens. Shown are median fluorescence intensities (MFI) of percent positive cells. MSCs were isolated and expanded in the bioreactor and analyzed at passage 0, passage 1, and higher passages (passage >1). Data are presented in whisker plots.

of MSCA-1 (1), whereas CD200 (6) showed marked increase at passage >1 and SSEA-4 (11,21) was present at low, yet ascending levels. Surface expression of CD271/NGFR (14) and CD349/Frizzled homolog 9 (5) displayed pronounced variability, but ultimately reduced values at passage >1. CD56/NCAM (1) showed pronounced variability in expression on cells at passage 1 or higher. CD117/c-kit was moderately expressed but also declined with progressing in vitro cultivation. Similarly, CD146 levels showed a marked decline on cells cultivated in vitro at higher passages.

These data demonstrate the donor-dependent variability of cellular expression pattern as well as the extensively published and controversially discussed heterogeneity of MSCs.

We were also interested in monitoring the cell surface profile to assess whether reciprocal interactions of MSCs with their microenvironment would be reflected

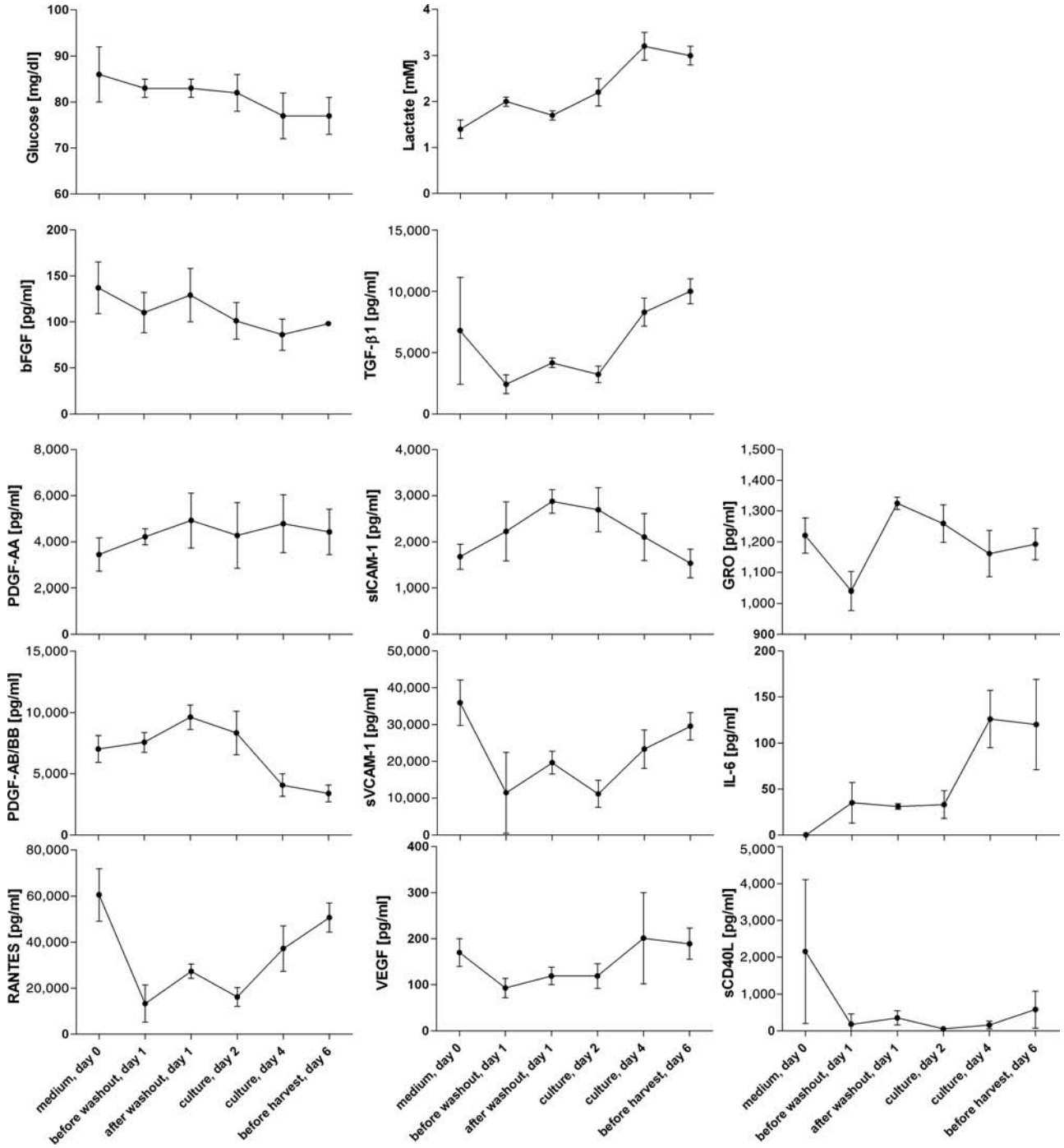

Figure 8. Cytokine analysis of culture medium in the bioreactor using preexpanded MSCs for cell expansion. Shown are mean and SD values of ($n = 3+$) measurements for glucose, lactate, basic fibroblast growth factor (bFGF), transforming growth factor (TGF)-β1, platelet-derived growth factor (PDGF)-AA, soluble intracellular adhesion molecule 1 (sICAM-1), growth regulated oncogene (GRO), PDGF-AB/BB, soluble vascular cell adhesion molecule 1 (sVCAM-1), interleukin-6 (IL-6), RANTES, VEGF, and soluble cluster of differentiation 40 ligand (sCD40L).

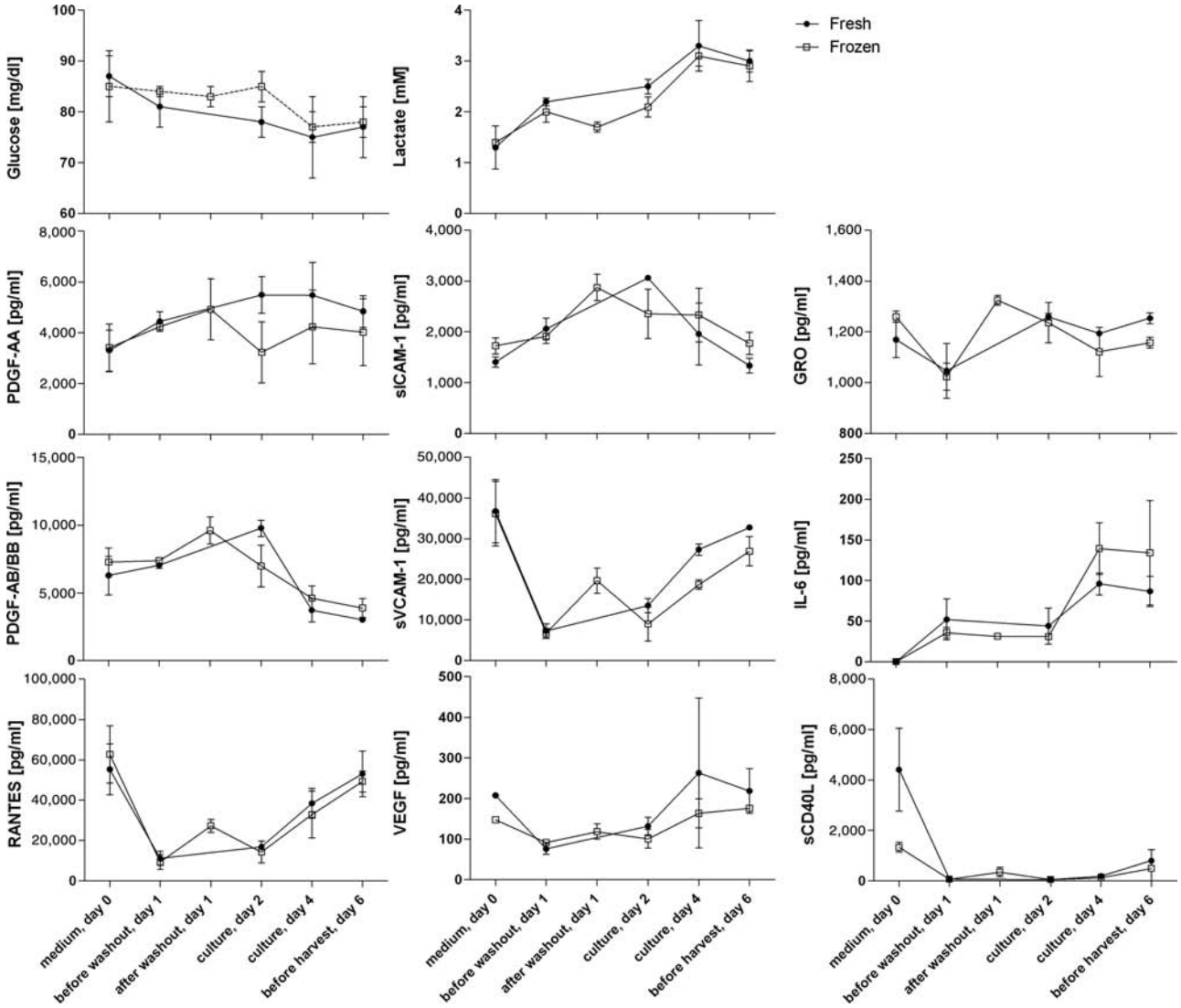

Figure 9. Cytokine quantification of cell culture medium. LUMINEX analysis of cell culture medium supernatants from the bioreactor using cryopreserved MSCs ("frozen") or nonmanipulated preexpanded cells ("fresh"). Shown are mean and SD values of $n=3$ cryopreserved (frozen) MSCs and $n=2$ preexpanded "fresh" cells.

in their receptor expression. In this regard, PDGF receptor α/CD140a was constitutively expressed at low levels, whereas PDGF receptor β/CD140b showed variable, yet strong expression, mirroring and underscoring our data examining the cytokine content in culture supernatant.

Interestingly, VEGF receptor/CD309 was expressed at very low levels and further declined subsequently whilst soluble VEGF concentrations showed some variability, but progressively ascended.

Finally, we wanted to investigate whether the effect of in vitro cell cultivation would modulate the surface expression profile of MSCs. MSCs have been shown to act as sentinels, sensing and reacting to attractants provided by inflammatory tissues, making them highly advantageous and attractive as a clinically relevant therapeutic. Functionally active MSCs should therefore be able to migrate to sites of ischemia or injury after systemic administration to exert their pleiotropic immunomodulatory effects. This entails a coordinated sequence of adhesion steps (22,30): (i) selectins and their ligands mediate cell tethering, (ii) captured cells roll on and further interact with the vessel wall, and finally (iii) chemokine-triggered activation of integrins will firmly bind and arrest the cell. Subsequently, transendothelial cell migration may occur.

Our flow cytometric analysis of chemokine receptors on the surface of MSCs revealed low expression of CCR1 (CD191) and CCR5 (CD195) and moderate and

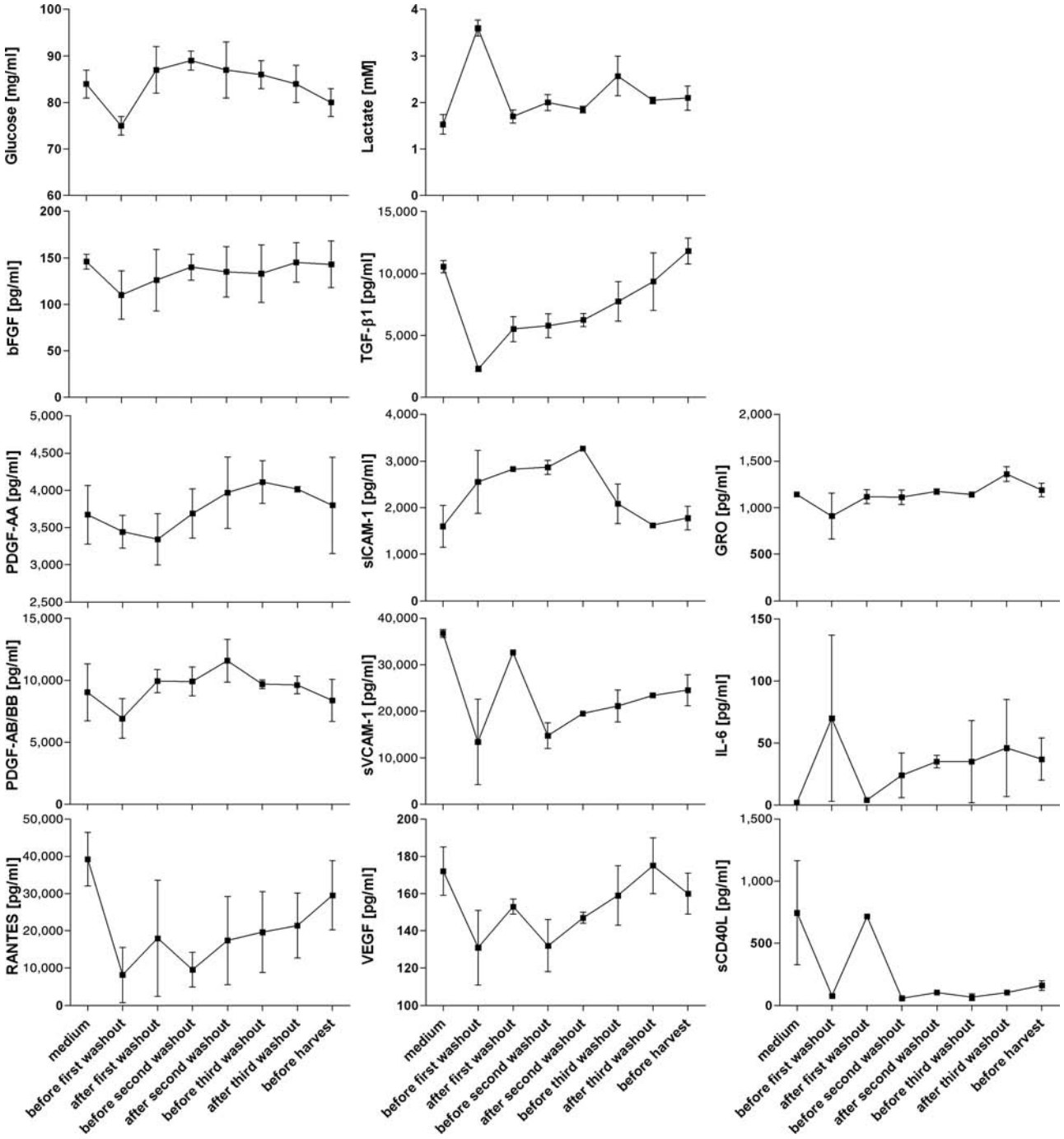

Figure 10. Analysis of metabolic markers and cytokines of culture medium from bioreactor using bone marrow to isolate and expand MSCs. Shown are mean and SD values of ($n = 1/2$) measurements for sICAM-1, sVCAM-1, and sCD40L as well as $n = 2/3$ for glucose, lactate, bFGF, TGF, PDGF-AA, GRO, PDGF-AB/BB, IL-6, RANTES, and VEGF. Note: No error bar is shown where $n < 3$.

variable levels of CCR3 (CD193), CCR4 (CD194), CCR7 (CD197), CXCR4, and CXCR7. Passaging of cells in the Quantum cell expansion system resulted in subsequent modification of these receptors, whereby CCR4 and CCR7 expression increased, and CCR3 and CXCR7 levels declined. In addition, we also analyzed the MSC surface profile of integrins CD29, CD49a, CD49c, CD49d, CD49e, CD49f, and CD51. Again, we could observe a highly dynamic modification of the expression profile on MSCs cultivated in the Quantum system, implying that the cells may respond to the mechanical and biological signals of their microenvironment. In this context,

we found a consistently high expression of the fibronectin receptor/CD49e on cells isolated and expanded in the Quantum system, possibly explaining the good expansion performance achieved with the fibronectin-coated bioreactors.

Notably, the modulation of surface receptor expression is no unique phenomenon of cells derived from the Quantum system, as similar results have been observed in conventional tissue culture as described by others (9,16,21). In summary, our comprehensive analysis of the MSC surface profile reflects the complex heterogeneity of the cell population cultivated in the Quantum system, documenting the presence of metabolic, chemotactic, and adhesive molecules on the cell surface.

The easiness of monitoring cellular metabolism in the Quantum system also offers an attractive advantage over conventional static tissue culture configurations due to higher homogeneity in the MSC culture by minimizing concentration gradients (pH, metabolites) and therefore preventing cell starvation in vitro. We investigated this unique feature by analyzing the cytokine and metabolite concentrations of culture media samples that were collected from fresh medium, pre- and post-washout, and before harvesting. These aliquots reflect the cell culture media composition and result from both supplemental factors and secreted molecules.

As previously documented (12), PL contains multiple growth factors as well as adhesion and signaling molecules, such as ICAM-1, GRO, PDGF-AA, PDGF-AB/BB, RANTES, VCAM-1, and VEGF. In addition, the ability of MSCs to secrete a range of bioactive molecules such as IL-6, TGF-β1, VEGF, PDGF-BB, etc., is now well documented (3,20,26). The cytokine profile of preexpanded MSCs cultivated in the Quantum system showing the cellular trophic activity substantiates these data and now also offers further insight into alterations of cytokine concentrations during MSC cultivation. Apart from known growth factors such as bFGF, TGF-β1, PDGF-AA, PDGF-AB/BB, RANTES, and VEGF, we also quantified adhesion molecules ICAM-1 and VCAM-1 and signaling molecules GRO (CXCL1/2/3), CD40L, and IL-6. Since MSCs may act at multiple stages of wound repair, clinical application of MSCs requires a multifunctional cellular population able to sense and react to external signals provided by sites of inflammation.

CXCL1 (GRO α), 2 (GRO β), and 3 (GRO γ) are three highly related chemokines (29) that bind to the same receptors but with differing affinities (23) and stimulate a number of biological responses including chemotaxis, angiogenesis, and growth regulation (29). GRO was found to be expressed by human cord blood-derived mesenchymal stem cells (CB-MSCs) (15) and to enhance CB-MSC migration (13). We found increasing levels of GRO in cell culture supernatants, suggesting also that the Quantum system-derived BM-MSCs may also secrete this factor. CD40 ligand (CD40L; CD154) is a member of the TNF superfamily and acts as a costimulatory molecule by binding to CD40 on antigen-presenting cells (APCs) in association with T-cell receptor stimulation by major histocompatibility complex (MHC) molecules on the APCs (18). CD40L is well known to be expressed by cells of the immune system but has also been found to be present in PL, declining rapidly in cell culture (12). Consistent with these data, we observed diminished CD40L concentrations in cell culture supernatant at day 1 compared to levels in fresh medium.

IL-6 is a central player in MSC-mediated immunomodulation, since it is induced by prostaglandin E2 (PGE2), but also positively regulates both cyclo-oxygenase 2 (COX2) and induced nitric oxide synthase (iNOS) activities (4). Moreover, it could be shown that IL-6 maintains the proliferative and undifferentiated state—their "stemness"—of bone marrow-derived MSCs by an extracellular signal-regulated kinase 1/2 (ERK1/2)-dependent mechanism (20). In accordance to these published data, we also observed a marked increase in IL-6 concentration during cell cultivation of MSCs.

Moreover, we investigated the metabolic state of cells during their in vitro culture period by measuring glucose and lactate levels to ascertain the feasibility and efficiency of the automated feeding process of the Quantum system. Regarding these metabolite concentrations, we could observe an increase in lactate during cell culture correlating with the measured glucose consumption, indicative of the metabolic cell activity of proliferating MSCs. However, glucose levels before harvest were still about 90% compared to levels in fresh medium, negating cell starvation.

The Quantum system is an integrated, closed system that can be used to efficiently expand MSCs in an automated, safe, and reproducible manner. It takes less floor space and requires less labor than manual systems, thereby allowing for larger-scale manufacturing of cells with less risk of contamination and better control of the process. In conclusion, the Quantum system reliably produces a cellular therapeutic dose and thus offers a readily available product. In the context of clinical application, the system may be further optimized by introducing GMP-compatible reagents for coating of the bioreactor and for supplementing the cell cultivation media. Moreover, as this functionally closed and automated system requires minimal manipulation, scalability is readily achieved by adding additional devices.

Our study demonstrates the capacity of both the Quantum bioreactor system and of our selected xeno-free medium formulations to enable the automated production of clinically relevant numbers of MSCs. In future studies, it will be critical to directly compare the function of MSCs manufactured in xeno-free media and in various bioreactor

configurations with the serum-containing T flask cultures that are being used in many ongoing clinical trials.

ACKNOWLEDGMENTS: We appreciate the excellent technical assistance of S. Chester, C. Späth, D. Erz, G. Baur, and T. Becker and the scientific and technical support of D. Windmiller. This work was supported by grants from the 7th Framework Program of the European Commission: CASCADE (Cultivated Adult Stem Cells as Alternative for Damaged tissuE) (HEALTH-F5-2009-223236) and REBORNE (REgenerating BOne defects using New biomedical Engineering approaches) (HEALTH-2009-1.4.2-241879) and the University Centre of Musculoskelettal Research, Ulm, Germany. M.T.R., N.F., D.F., J.D., and H.S. work for a nonprofit organization that is producing and marketing platelet lysate. S.B., K.N., and D.A. work for TerumoBCT that has developed and is producing and marketing Quantum cell expansion system. This publication forms part of the Ph.D. thesis of N. Fekete at the University of Ulm. Contribution: M.T.R., J.D., D.A., H.S., S.B., L.S., and K.N. planned and M.T.R. and J.D. performed MSC expansions in Quantum system and T-25. N.F. and M.T.R. did flow cytometry and wrote the manuscript. D.A. instructed MSC work using Quantum system. N.F. and D.F. analyzed chemokine and cytokine patterns. M.T.R., L.K., and A.I. differentiated MSCs.

REFERENCES

1. Battula, V. L.; Treml, S.; Bareiss, P. M.; Gieseke, F.; Roelofs, H.; de Zwart, P.; Muller, I.; Schewe, B.; Skutella, T.; Fibbe, W. E.; Kanz, L.; Buhring, H. J. Isolation of functionally distinct mesenchymal stem cell subsets using antibodies against CD56, CD271, and mesenchymal stem cell antigen-1. Haematologica 94(2):173–184; 2009.
2. Bernardo, M. E.; Cometa, A. M.; Pagliara, D.; Vinti, L.; Rossi, F.; Cristantielli, R.; Palumbo, G.; Locatelli, F. Ex vivo expansion of mesenchymal stromal cells. Best Pract. Res. Clin. Haematol. 24(1):73–81; 2011.
3. Bieback, K.; Schallmoser, K.; Klüter, H.; Strunk, D. Clinical protocols for the isolation and expansion of mesenchymal stromal cells. Transfus. Med. Hemother. 35(4):286–294; 2008.
4. Bouffi, C.; Bony, C.; Courties, G.; Jorgensen, C.; Noel, D. IL-6-dependent PGE2 secretion by mesenchymal stem cells inhibits local inflammation in experimental arthritis. PLoS One 5(12):e14247; 2010.
5. Buhring, H. J.; Battula, V. L.; Treml, S.; Schewe, B.; Kanz, L.; Vogel, W. Novel markers for the prospective isolation of human MSC. Ann. N.Y. Acad. Sci. 1106:262–271; 2007.
6. Buhring, H. J.; Treml, S.; Cerabona, F.; de Zwart, P.; Kanz, L.; Sobiesiak, M. Phenotypic characterization of distinct human bone marrow-derived MSC subsets. Ann. N.Y. Acad. Sci. 1176:124–134; 2009.
7. Caplan, A. I. Adult mesenchymal stem cells for tissue engineering versus regenerative medicine. J. Cell. Physiol. 213(2):341–347; 2007.
8. Caplan, A. I. The mesengenic process. Clin. Plast. Surg. 21(3):429–435; 1994.
9. Ciuculescu, F.; Giesen, M.; Deak, E.; Lang, V.; Seifried, E.; Henschler, R. Variability in chemokine-induced adhesion of human mesenchymal stromal cells. Cytotherapy 13(10): 1172–1179; 2011.
10. Dominici, M.; Le Blanc, K.; Mueller, I.; Slaper-Cortenbach, I.; Marini, F.; Krause, D.; Deans, R.; Keating, A.; Prockop, D.; Horwitz, E. Minimal criteria for defining multipotent mesenchymal stromal cells. The International Society for Cellular Therapy position statement. Cytotherapy 8(4):315–317; 2006.
11. Fazzi, R.; Pacini, S.; Carnicelli, V.; Trombi, L.; Montali, M.; Lazzarini, E.; Petrini, M. Mesodermal progenitor cells (MPCs) Differentiate into mesenchymal stromal cells (MSCs) by activation of Wnt5/calmodulin signalling pathway. PLoS One 6(9):e25600; 2011.
12. Fekete, N.; Gadelorge, M.; Furst, D.; Maurer, C.; Dausend, J.; Fleury-Cappellesso, S.; Mailander, V.; Lotfi, R.; Ignatius, A.; Sensebe, L.; Bourin, P.; Schrezenmeier, H.; Rojewski, M. T. Platelet lysate from whole blood-derived pooled platelet concentrates and apheresis-derived platelet concentrates for the isolation and expansion of human bone marrow mesenchymal stromal cells: Production process, content and identification of active components. Cytotherapy 14(5):540–554; 2012.
13. Kim, D. S.; Kim, J. H.; Lee, J. K.; Choi, S. J.; Kim, J. S.; Jeun, S. S.; Oh, W.; Yang, Y. S.; Chang, J. W. Overexpression of CXC chemokine receptors is required for the superior glioma-tracking property of umbilical cord blood-derived mesenchymal stem cells. Stem Cells Dev. 18(3):511–519; 2009.
14. Kuci, S.; Kuci, Z.; Kreyenberg, H.; Deak, E.; Putsch, K.; Huenecke, S.; Amara, C.; Koller, S.; Rettinger, E.; Grez, M.; Koehl, U.; Latifi-Pupovci, H.; Henschler, R.; Tonn, T.; von, L. D.; Klingebiel, T.; Bader, P. CD271 antigen defines a subset of multipotent stromal cells with immunosuppressive and lymphohematopoietic engraftment-promoting properties. Haematologica 95(4):651–659; 2010.
15. Liu, C. H.; Hwang, S. M. Cytokine interactions in mesenchymal stem cells from cord blood. Cytokine 32(6):270–279; 2005.
16. Mafi, R.; Hindocha, S.; Mafi, P.; Griffin, M.; Khan, W. S. Sources of adult mesenchymal stem cells applicable for musculoskeletal applications—a systematic review of the literature. Open Orthop. J. 5(Suppl 2):242–248; 2011.
17. Nguyen, K.; Brecheiesen, M.; Peters, R.; Startz, T.; Vang, B.; Baila, S. Quantum® cell expansion system—automated expansion of human mesenchymal stem cells from precultured cells using the Quantum cell expansion system. TERUMO BCT:http://www.terumobct.com/location/north-america/Documents/THX_Quantum_MSC_WP_8.5x11_V12_14.pdf; 2012.
18. Peters, A. L.; Stunz, L. L.; Bishop, G. A. CD40 and autoimmunity: The dark side of a great activator. Semin. Immunol. 21(5):293–300; 2009.
19. Phinney, D. G.; Kopen, G.; Righter, W.; Webster, S.; Tremain, N.; Prockop, D. J. Donor variation in the growth properties and osteogenic potential of human marrow stromal cells. J. Cell. Biochem. 75(3):424–436; 1999.
20. Pricola, K. L.; Kuhn, N. Z.; Haleem-Smith, H.; Song, Y.; Tuan, R. S. Interleukin-6 maintains bone marrow-derived mesenchymal stem cell stemness by an ERK1/2-dependent mechanism. J. Cell. Biochem. 108(3):577–588; 2009.
21. Rojewski, M. T.; Weber, B. M.; Schrezenmeier, H. Phenotypic characterization of mesenchymal stem cells from various tissues. Transfus. Med. Hemother. 35(3):168–184; 2008.
22. Ruster, B.; Gottig, S.; Ludwig, R. J.; Bistrian, R.; Muller, S.; Seifried, E.; Gille, J.; Henschler, R. Mesenchymal stem cells display coordinated rolling and adhesion behavior on endothelial cells. Blood 108(12):3938–3944; 2006.

23. Schumacher, C.; Clark-Lewis, I.; Baggiolini, M.; Moser, B. High- and low-affinity binding of GRO α and neutrophil-activating peptide 2 to interleukin-8 receptors on human neutrophils. Proc. Natl. Acad. Sci. USA 89(21):10542–10546; 1992.
24. Siddappa, R.; Licht, R.; van Blitterswijk, C.; de Boer, J. Donor variation and loss of multipotency during in vitro expansion of human mesenchymal stem cells for bone tissue engineering. J. Orthop. Res. 25(8):1029–1041; 2007.
25. Singer, N. G.; Caplan, A. I. Mesenchymal stem cells: Mechanisms of inflammation. Ann. Rev. Pathol. Mech. Dis. 6(1):457–478; 2011.
26. Spaeth, E. L.; Dembinski, J. L.; Sasser, A. K.; Watson, K.; Klopp, A.; Hall, B.; Andreeff, M.; Marini, F. Mesenchymal stem cell transition to tumor-associated fibroblasts contributes to fibrovascular network expansion and tumor progression. PLoS One 4(4):e4992; 2009.
27. Subbanna, P. K. T. Mesenchymal stem cells for treating GVHD: In vivo fate and optimal dose. Med. Hypotheses 69(2):469–470; 2007.
28. Tautzenberger, A.; Lorenz, S.; Kreja, L.; Zeller, A.; Musyanovych, A.; Schrezenmeier, H.; Landfester, K.; Mailander, V.; Ignatius, A. Effect of functionalised fluorescence-labelled nanoparticles on mesenchymal stem cell differentiation. Biomaterials 31(8):2064–2071; 2010.
29. Wuyts, A.; Govaerts, C.; Struyf, S.; Lenaerts, J. P.; Put, W.; Conings, R.; Proost, P.; Van Damme, J. Isolation of the CXC chemokines ENA-78, GRO α and GRO γ from tumor cells and leukocytes reveals NH2-terminal heterogeneity. Functional comparison of different natural isoforms. Eur. J. Biochem. 260(2):421–429; 1999.
30. Yagi, H.; Soto-Gutierrez, A.; Parekkadan, B.; Kitagawa, Y.; Tompkins, R. G.; Kobayashi, N.; Yarmush, M. L. Mesenchymal stem cells: Mechanisms of immunomodulation and homing. Cell Transplant. 19(6):667–679; 2010.